few to 10 MPa and are thus likely to survive re-impact. If such a clast does survive, it may continue on an escape trajectory if the re-impact is at a grazing angle and the local escape velocity at the point of first contact is less than that at the initial launch point. Alternatively, the clast may lose enough energy to cause it to follow a non-escape trajectory subsequently, thus bouncing one or more times (Fig. 2; compare to lunar boulder tracks in Fig. 1f–g; see also Fig. 13). The number of bounces, the spacing between the contacts, and the ultimate fate of the clast again depend critically on the material properties of the clast and that portion of the surface with which it interacts. Depending on the size of the clast, the fate of the clast may be 1) effectively an assemblage of relatively small regolith particles, 2) a mixture of clast sizes approaching that of the impacting clast, or 3) a single clast supported by a regolith matrix.

Of even more interest are sub-orbital ejecta clasts that leave the crater cavity at speeds of 3–8 m s^{-1} (i.e., just less than or almost equal to the local escape velocity) and at elevation angles close to zero (Fig. 2). Such clasts will travel out of the crater, over the crater rim crest, and onto the crater rim in the terminal stages of the cratering event and may slide, roll, or bounce along the surface, producing a groove-like disturbance of the surface that is narrower than, or similar to, their own diameter. High-resolution images of the lunar surface have shown many examples of such features (Fig. 1f–g; see also Fig. 13), which include grooves, pitted grooves, and associated boulders in isolation or in association with impact craters (Moore, 1970; Mitchell et al., 1973; Muehlberger et al., 1973). Boulder tracks were investigated in detail by the Apollo 17 astronauts (Schmitt and Cernan, 1973) (Fig. 1f–g). We now concentrate on the fate of suborbital ejecta clasts that leave the interior and the rim crest of the crater Stickney at elevation angles near zero.

When considering the motion of an ejecta clast launched essentially tangential to the surface of Phobos it is convenient to resolve the problem into two aspects. The first is that the width and depth of a groove are related to the gravitational weight of the ejecta clast and the cohesive strength of the regolith via the balance of vertical forces. The second aspect concerns the horizontal motion of the clast. It must have a sufficient initial kinetic energy reservoir to supply both the mechanical energy needed to overcome the bonding strength of regolith particles in its path as they are disaggregated and the potential energy needed to deposit these loose particles into a groove rim (where one forms). Whether or not a rim is formed, energy is also needed to compact the regolith as the boulder (i.e., clast) passes. We treat these two aspects of the problem in turn.

3. Groove depth and width

The static aspects of a regolith supporting a large clast have been addressed for lunar boulders by Moore (1970) using basic soil-mechanics equations from Terzaghi and Peck (1948, 1967). If a clast (considered for simplicity to be spherical) with radius r and density ρ_b sinks by an amount D_f into a regolith of density ρ_r and cohesive strength C in such a way that the horizontal contact area is πR_f^2, then on a body where the acceleration due to gravity is g, the balance of forces is such that

$$\frac{4}{3}\pi r^3 \rho_b g = \left(\pi R_f^2\right)\left[1.3 N_c C + \rho_r g\left(N_q D_f + 0.6 N_g R_f\right)\right], \quad (1)$$

where N_c, N_q, and N_g are dimensionless constants that depend mainly on the internal friction angle of the regolith material, ϕ, and its general state of compaction. Internal friction angles for the lunar regolith are found by various methods to range from 10–30° for regions where boulder tracks were seen in Lunar Orbiter images (Moore, 1970) and from 26–50° for surface experiments at the Apollo 17 site (Mitchell et al., 1973). Here, we explore the consequences of varying ϕ from 25° to 35°. Data given by Terzaghi and Peck (1967, page 222) then imply that, for $\phi=25°$, $N_c=24.5$, $N_q=12.5$, and $N_g=10.0$; for $\phi=30°$, $N_c=36.75$, $N_q=21.5$, and $N_g=20.0$; and for $\phi=35°$, $N_c=58.0$, $N_q=40.5$, and $N_g=43.0$.

We can establish a relationship between r, R_f, and D_f, using the fact that a groove produced by a spherical boulder can be approximated by the cross-sectional shape of a circular segment. Then, if $R_f=f\,r$ and $D_f=q\,r$, simple algebra relating the chord and radius of a circle shows that

$$f = \left(2q - q^2\right)^{1/2}. \quad (2)$$

It is convenient to introduce the easily measured depth/width ratio a where $a=[D_f/(2R_f)]$. Additional algebra shows that

$$q = \frac{8a^2}{1+4a^2}. \quad (3)$$

The variations of f and q with respect to a are shown in Fig. 3. Rearranging Eq. (1), we have

$$C = \left(\frac{r\,g}{1.3\,N_c}\right)\left[\frac{4}{3f^2}\rho_b - \left(N_q\,q + 0.6\,N_g\,f\right)\right]\rho_r. \quad (4)$$

For given values of boulder radius, r, the local effective acceleration due to gravity, g, boulder and regolith densities, ρ_b and ρ_r, respectively, and a choice of internal friction angle, ϕ (and hence values of N_c, N_q and N_g), this equation gives C as a function of a, because q can be found as a function of a using (3) and f can be found from q using (2). We take $\rho_b=1800$ kg m^{-3}, a density close to the bulk density of Phobos (1876 kg m^{-3}: Andert et al., 2010), and use values of $\rho_r=800$, 1000, and 1200 kg m^{-3} based on the assumption that the regolith density will be somewhat less on Phobos than on the Moon (for which $\rho_r \sim 1500$–1600 kg m^{-3}: Mitchell et al., 1973; Kuzmin et al., 2003). We use 5.7×10^{-3} ms^{-2} as the effective acceleration due to gravity, the global average corresponding to the current best estimate of the density of Phobos (P. C. Thomas, personal communication; Shi et al., 2011; Willner et al., 2011). Examples of the variation of cohesive strength, C, with depth-to-width ratio, a, are shown in Fig. 4a for a fixed boulder radius, r, of 150 m and internal friction angles $\phi=25°$, 30°, and 35°, and in Fig. 4b for r of 50, 150, and 250 m for $\phi=30°$. The boulder radii are chosen on the basis of arguments presented later in this section.

A number of results follow from Fig. 4. For each value of regolith density, ρ_r, there is a limiting value of a above which the implied value of C is negative. This means that, even if the regolith

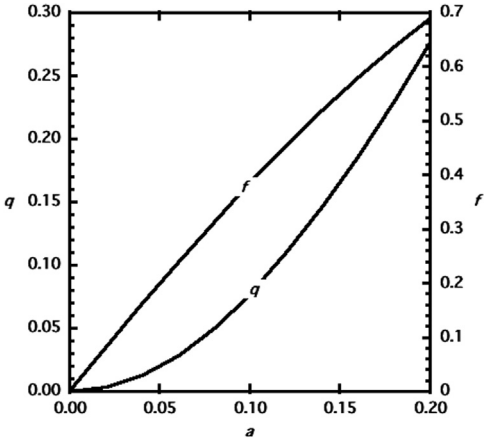

Fig. 3. The variations of the dimensionless parameters f and q with clast track depth–width aspect ratio a, given by Eqs. (2) and (3).